



Effect of CO₂ Laser Fluence on Cladding Geometrical Dimensions Alternations

Mohammed J. Kadhim^a, Mahdi M. Hanon^b, Suhair A. Hussein^{c*}

^a Department of Production Engineering and Metallurgy, University of Technology, Baghdad, Iraq

^b Department of Production Engineering and Metallurgy, University of Technology, Baghdad, Iraq

^c Department of Production Engineering and Metallurgy, University of Technology, Baghdad, Iraq,
zainzain2011.zz@gmail.com

* Corresponding author.

Submitted: 04/12/2019

Accepted: 03/08/2020

Published: 25/05/2021

KEYWORDS

Clad Geometrical Dimensions, Dilution Area, Cladding Width, Dilution Percentage, Depth of Dilution.

ABSTRACT

Geometrical dimensions could play a potential role in the function of laser cladding of nickel-base powder on the cold-rolled carbon steel substrate. The geometrical dimensions and their impact on the efficiency of the process of laser cladding of nickel-base powder (Ni -10wt% Al) on cold rolled 0.2% carbon steel substrate was investigated. This work focused on the effect of laser-specific energy input of CO₂ laser. The geometrical dimensions of cladding regions are including cladding width, cladding height, depth of dilution, contact angle, dilution area, cladding area, and heat-affected zone dimensions determinations. The laser power (1.8 kW) was used at different traverse speeds (1.5, 3.6, 5, 7.1, 8.6, 12.5 mm/s) with (3mm) laser beam diameter. The feed rate was kept constant after many preliminary claddings at approximately 11 g/min. Fluence values ranged from (48-400J/mm²), and the power density value was (255W/mm²). A minimum dilution percentage (25%) was obtained at the highest fluence value (400 J/mm²). Observations were measured using an optical microscope, scanning electron microscopy, and Image software. Obtained results indicated that the increase in the fluence leads to an increase in height of cladding, HAZ region but lower depth of dilution.

How to cite this article: M. J. Kadhim, M. M. Hanon, S. A. Hussein, "Effect of CO₂ laser fluence on cladding geometrical dimensions alternations," Engineering and Technology Journal, Vol. 39, Part A, No. 05, pp. 703-710, 2021. DOI: <https://doi.org/10.30684/etj.v39i5A.1474>

This is an open access article under the CC BY 4.0 license (<http://creativecommons.org/licenses/by/4.0>).

1. INTRODUCTION

Laser cladding can be characterized as a melting procedure in which the laser beam prompt to fuse an alloy addition onto a substrate (base material) producing a homogeneous surface with solid metallurgical bonding on the substrate with very low dilution [1]. Today, in the manufacturing business, the importance of CO₂ laser cladding process is represented by its efficiency to increase the resistance of surfaces with saving cost, time, and effort by the deposition of a powder on the substrate [2]. This leads to many fields that go to increase the utilization, this process with diversity materials parts is used according to the required properties.

Amongst the laser technology applications, cladding laser received significant concern in the latest years because of its various material processing potentials, such as metals coating, repairing high-value components, prototyping, and manufacturing low-volume [3]. The cladding laser process can produce a much better covering and better surface quality with less distortion and minimum dilution [4]. Also, there are many benefits to using this process as a swift prototyping mechanism. Fast prototyping can be used for producing mechanical parts in a layered pattern, which allows the part fabrication with distinctive features to prototyping laser cladding, producing a homogeneous structure and enhance mechanical characteristics and produce multiplex geometries [5].

The most significant structural alloys widely used for many applications which require medium mechanical properties and chemical stability are low carbon steels [6]. These materials may be considered as important cheap substrates for the deposition of clad coatings for many high corrosion and oxidation resistance alloys such as Ni-Al alloys [7].

P. Chiu [8] studied the 50 W CO₂ laser cladding with powders of 304L coating on the substrate of stainless steel. At cladding vertically from the stainless steel (substrate), the heat of the following layer is transferred to the sample. A high amount of powder was deposited when the speed of cladding was less than 20 mm/min which formed 2 mm of cladding width. The speed changing from 20-30 mm/min enhances the avoidance of the insufficient adhesion for powder. Tuncay Simsek [9] investigated nanoparticles of titanium carbide (TiC) covering the substrate of X40CrMoV51 (H13) hot work tool steel with 2000 W by CO₂ laser cladding process. The most successful covering was obtained at a thickness of cladding 130 μm. The hardness enhancements are nearly three times higher than the substrate. Also, the wear resistance increased when the cladding surface was exposed to scratching.

This research using a cheap substrate of cold-rolled 0.2 wt% carbon steel and cladding it with Ni- 10 wt% Al powder by using a high-power carbon dioxide laser process to study how the dimensional geometries of clad regions can be affected according to different values of specific energies. Higher cladding area with lower dilution percentage obtained when the influence was 400J/mm² without defects.

2. EXPERIMENTAL PROCEDURES

Flat plates of cold-rolled 0.2 wt% carbon steel of thickness 6 mm, width 30 mm, and length 60 mm were used as a substrate for laser cladding. To achieve high absorption of the substrate to CO₂ laser beam, critical preparations were made to the substrate before laser cladding. The substrates were sandblasted to produce a relatively rough surface of approximately 10 μm CLA roughness to enhance the absorption. The sample was then thoroughly cleaned with alcohol and acetone and coated with a thin layer of carbon dag to increase higher the absorptivity. The clad powder used is a thorough mixture of 90wt% Ni and 10 wt% Al. The average particle size of Ni and Al powders are 106 and 250 μm, respectively.

The samples to be cladded at 1.8 kW continuous, fast axial, shock stabilized, gas discharged CO₂ laser model BOC 901 which was designed by British Oxygen Company and manufactured by Control Laser Ltd. The laser beam of 10.6 μm wavelength is produced from the mixture of CO₂, He, and N₂ gases entered the four tubes. These gases moved inside the tubes transferred to the plasma by using a Root Blower to produce the laser beam. These gases are drawn at a high speed of approximately 500 m/s, and high pressure of approximately 35tor. These conditions are sufficient to generate a stable discharge and shock wave to the gases in the state of plasma to produce a field of power supply to the tubes. The gases inside the tubes are excited electrically at 30 kV and a total current for all tubes of 600 mA. More details regarding the laser formation are out of this thesis. The mixture of gases is 5-10% CO₂, 10-15 N₂, and 75-85% He. The pumping of the gas mixture is taken

place at 1 atmospheric pressure. The approximate laser beam diameter excited from the partially reflected ZnSe mirror is 20 mm (approximately 35% for the CO₂ wavelength, 10.6 μm). This laser beam was reflected from the 45° stationary inclined gold-coated copper mirror through the laser head (Figure 1). The reflected beam is entered the laser head vertically to focus near the nozzle to approximately 0.4 mm. The laser beam was focused using 150 mm bi-convex KCl lens using suitable spacers to achieve the focused beam near the outer surface of the copper nozzle. The main reason for using KCl lens is the transmission of 10.6 μm CO₂ wavelength laser beam.

The feed rate was kept constant after many preliminary claddings at approximately 11 g/min. To produce clads with different specific energies and interaction times, different traverse speeds were used in the range of 1.5 to 12.5 mm/s (TABLE I). The laser power used to produce a high-power density suitable for laser cladding (power/laser beam area) and different specific energies is 1.8 kW. The laser mode tuned is near TEM₀₀.

The clad samples were cut by wire cutting transversally and then grinding with 220,500 and 1000 SiC grid emery papers respectively and then polished with 1 μm diamond paste and dried. Two etching solutions were used to evaluate the microstructure of (i) substrate and heat-affected zones; Nital (98% Alcohol +2% HNO₃) and (ii) the cladding area with 3ml HCl, 2ml HNO₃, and 0.1 ml glycerin.

It is very important to determine the % area dilution [10] which is equal to the melted area beneath the substrate to the total area of cladding. The area dilution was determined using Image J software. The dimensions such as laser cladding width, laser cladding height, depth of dilution, total clad thickness, HAZ, and contact angles were measured from the transverse sections. The prepared laser clads were inspected metal graphically utilizing standard metallography strategies for optical and SEM type vega3 test scan (Figure 1).

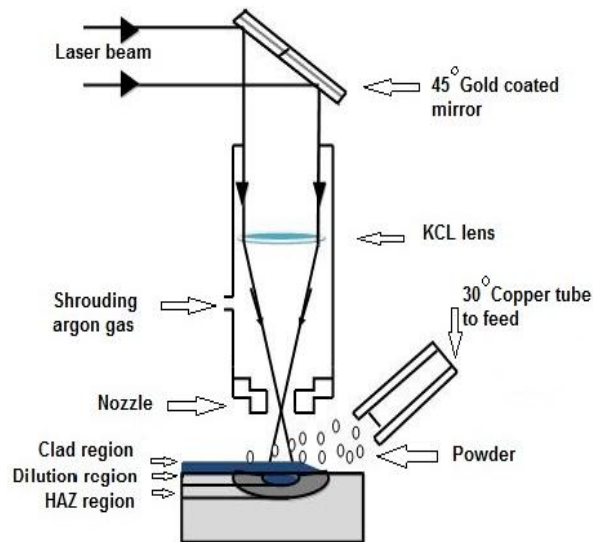


Figure 1: Some laser cladding system components.

TABLE I: The most important parameters of cladding process.

Parameters	values
TEM _{mn}	00
Raw laser beam diameter	20mm
Focal length	125mm
Shrouding gas ,Argon	2.2 SLPM
Laser power (P)	1.8 kW
Laser beam diameter (d)	3mm
Traverse speed (V)	1.5-12.5 mm/s
Interacton time (t)	0.24-2 s
Power density ($4P/\pi d^2$)	255W/mm ²
Fluence (P/dv)	48-400 J/mm ²

2. RESULTS AND DISCUSSION

After a cold rolled 0.2% carbon steel has been clad with Ni – 10 wt% Al powder at different values of fluence many features are produced at any cladding laser coatings. No cracking was observed at the cladding under all values of fluence used. Carefully measured for the different dimensional geometries illustrated by (Figure 2). The different dimensions of the clad region can be expressed as; W: is the width of laser cladding, H: is laser cladding height, D is dilution depth, T: is the total thickness of clad (H+D), HAZ: heat-affected zone, and C: is the contact angle (TABLE II). The variation of cladding dimension with the fluence is shown in Figure 3.

TABLE II: The dimensional geometry according to different values of fluence.

No. of samples	V Mm /s	fluence J/mm ²	W μm	H μm	D μm	T (H+D) μm	HA Z μm	Dilution Area μm ²	Cladding Area μm ²	Dilution Percentage	C Degree
1	1.5	400	960	256	63	319	277	1743	5003	25	43
2	3.6	167	1008	192	41	233	345	1912	4494	29	40
3	5	120	988	132	65	179	317	1667	3392	32	26
4	7.1	85	920	79	71	150	236	1591	1965	44	13
5	8.6	70	621	41	23	64	194	1911	1488	56	7
6	12.5	48	607	29	12	41	164	1698	1035	62	4

This table showed the succeeded laser clad regions that can be gained with increasing fluency to 400 J/mm². It was able to produce a thick cladding height of approximately 256 μm with lower dilution 63 μm at higher fluence due to low traverse speed and high interaction time with lower dilution. It should be mentioned that the relatively small cladding width at the highest fluence 400 J/mm² is due to increasing cladding height. Also, the value of depth of dilution was minimum at the lowest fluence compared with the highest fluence value is due to cladding height.

It is possible to notice the increasing the of HAZ regions with increasing the fluence value was due to increased height of cladding and lower the depth of dilution with the correlation of the fluence (Figure 4). The relationship between contact angle and fluency was found (Figure 5). This is related to the flow of cladding alloy as a function of specific energy. The contact angle was increased with increasing fluence (correlated with the higher interaction of time and decreasing the scanning speed), this expanding of contact angle is due to highly increasing the solid/liquid component of the clad region [12].

It is very important to measure the dilution percentage because of its effect on the strong bonding between the substrate and clad powder [13]. Generally, increasing the dilution percentage means that the strength bonding increased too. The percentage of dilution increased with the decrease of fluency; this is due to the increasing traverse speed of cladding (Figure 6) [14]. On the other hand, the percentage of dilution elevated directly with raising the traverse speed of cladding, this can be demonstrated, when the traverse speed of cladding is low the melt penetration is high. But, due to the high thickness of cladding, this leads to a decrease in the melting substrate which results in the occurrence of a minimum mixing between clad powder and substrate (Figure7) [15]. Briefly, one can link what happened to the height of cladding if the decrease of the melting in the substrate increased, that means the mixing between of substrate and the powder of cladding increased, and therefore the dilution increased. SEM analysis shows the details of the upper cladding region (Figure 8). EDS analysis proved that the center of the substrate region mainly containing from Fe while the region near the interface is composed of Fe, Ni, and Al (Figure 9). The fluence can be considered as a function of dimensional geometries in the laser cladding process [11].

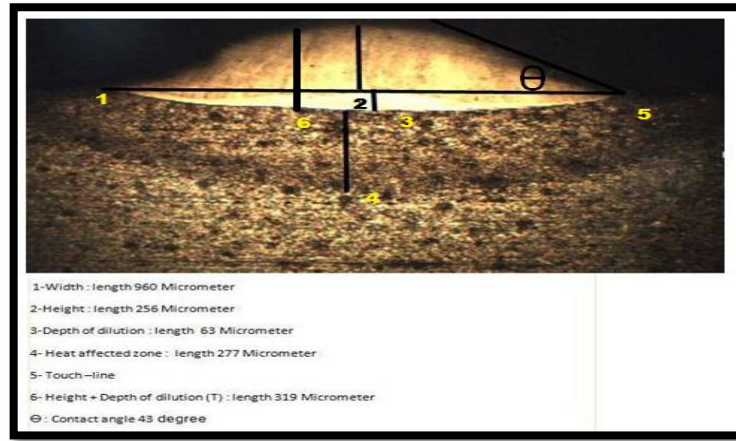


Figure 2: Six dimensions measured in electron microscopy.

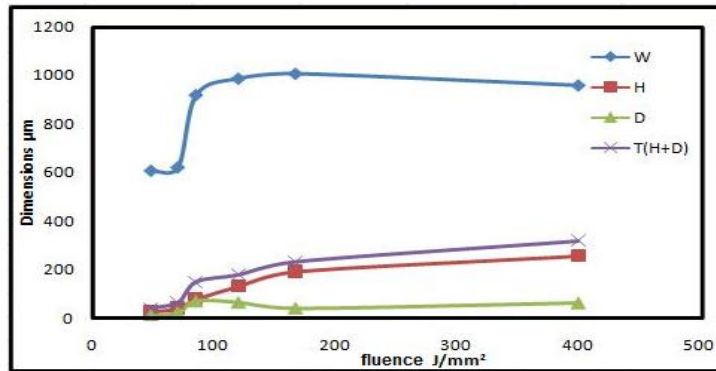


Figure 3: Relationships between cladding dimensions and fluence.

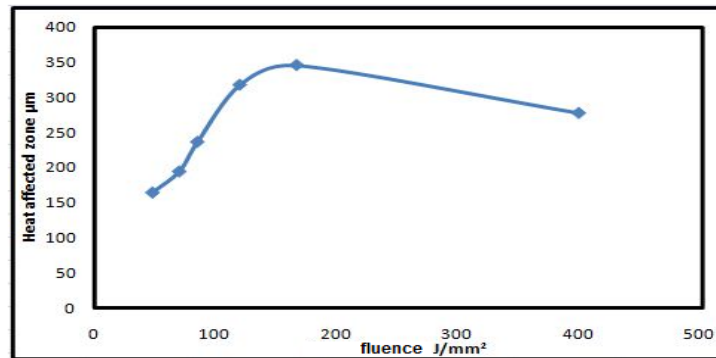


Figure 4: Relationship between heat affected zone and fluence.

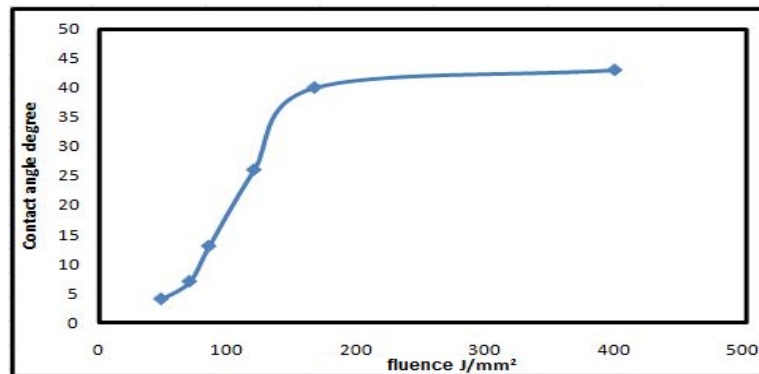


Figure 5: The relationship between contact angle and fluence.

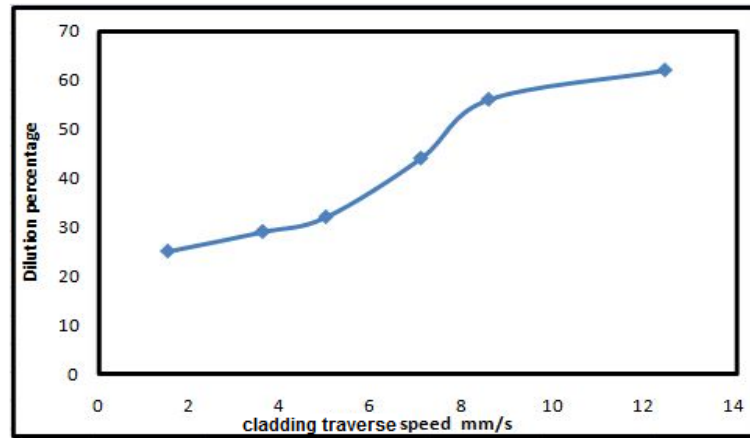


Figure 6: Relationship between dilution percentage and cladding traverse speed.

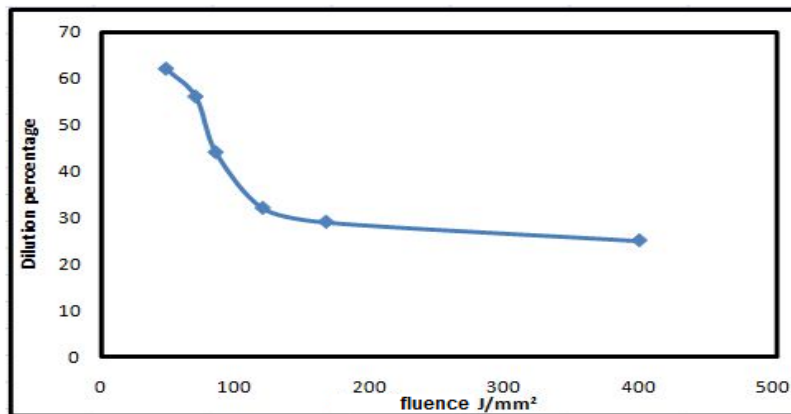


Figure 7: Relationship between dilution percentage and fluence.

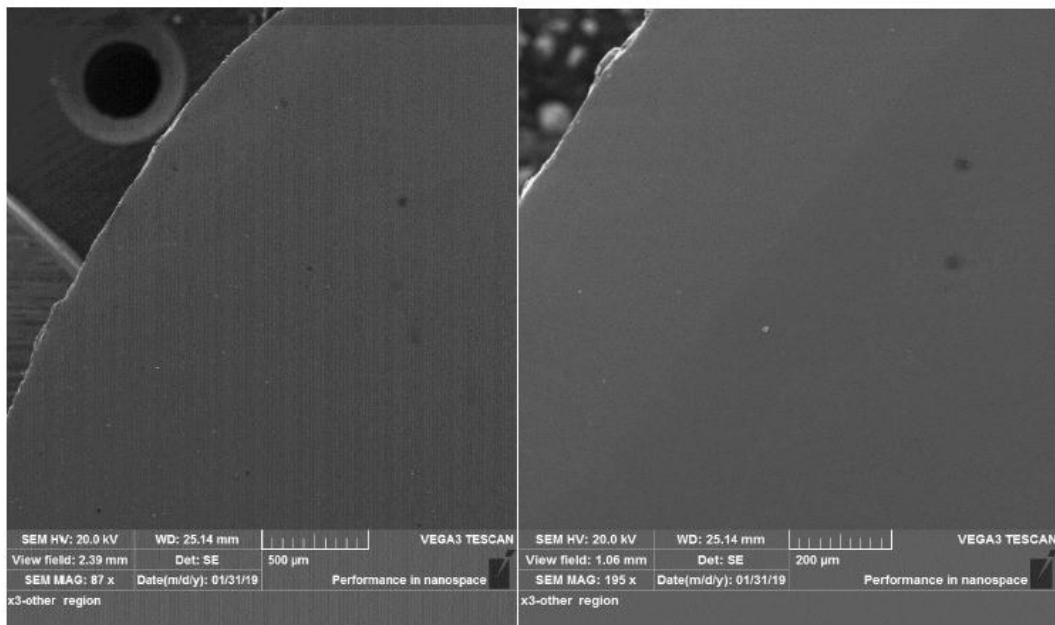


Figure 8: SEM micrographs of the upper cladding coating.

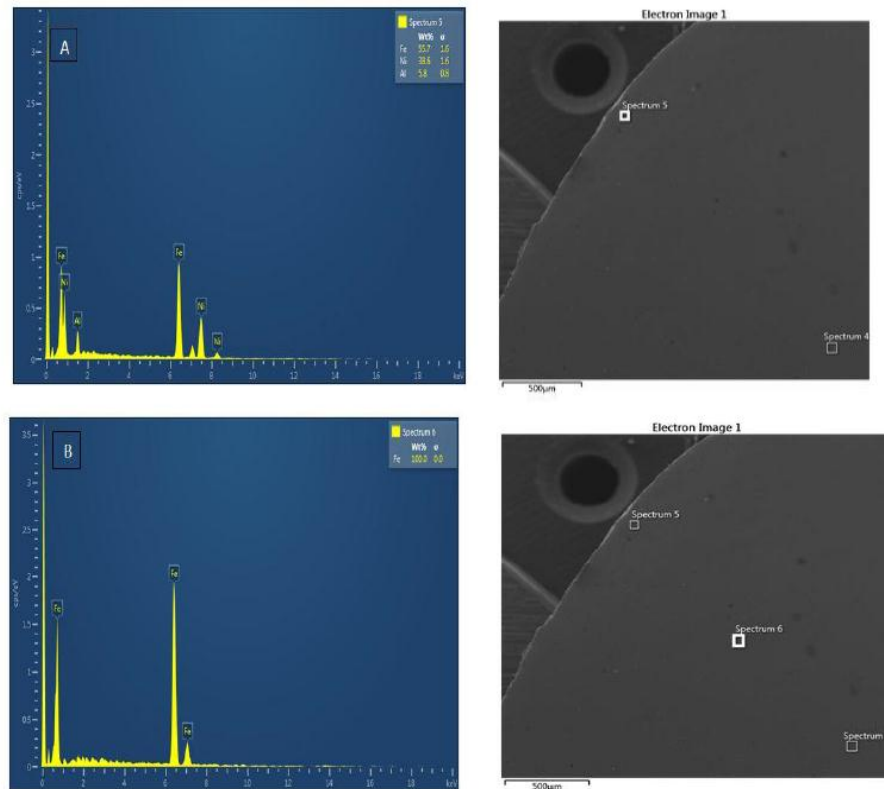


Figure 9: EDS analysis: A- near the interface B- the center of the substrate.

3. CONCLUSIONS

- 1) High power CO₂ laser cladding cold rolled 0.2 % carbon steel substrate with 90wt% Ni and 10 wt% Al powder is feasible to produce a high-quality surface layer.
- 2) Laser cladding experiments of single tracks indicate with fluence from 48-400 J/mm² and clad thickness from 41-319 µm can be obtained.
- 3) The results showed that the dilution dependent on cladding traverse speed according to the constant of other variables of the laser cladding process.
- 4) The dimensional geometries of cladding regions depend on the fluence.

References

- [1] L. Jianli, Y. Huijun, C. Chuanzhong, W. Fei, D. Jingjie, "Research and development status of laser cladding on magnesium alloys: A review," *Optics and Lasers in Eng.*, Vol. 93, pp. 195-210, 2017.
- [2] E. M. Birger, G. V. Moskvitin, A. N. Polyakov, "Industrial laser cladding: current state and future," *Welding International*, Vol. 25, No. 03, pp. 234-243, 2011.
- [3] J. Y. Jeng, S. C. Peng, J. Chou, "Metal rapid prototype fabrication using selective laser cladding technology," *The International Journal of Advanced Manufacturing Technology*, Vol. 16, No. 9, pp. 681-687, 2000.
- [4] C. Navas, A. Conde, B. J. Fernandez, "Laser coatings to improve wear resistance of mould steel," *Surface and Coatings Technology*, Vol. 194, No. 1, pp. 136-142, 2005.
- [5] D. J. Richardson, J. Nilsson, and W. A. Clarkson, "High power fiber lasers: current status and future perspectives," *Journal of the Optical Society of America B*, Vol. 27, No. 11, pp. B63-B92, 2011.
- [6] Kim, Hansoo, Dong-Woo Suh, and Nack J. Kim, Fe-Al-Mn-C lightweight structural alloys: a review on the microstructures and mechanical properties, *Science and Technology of Advanced Materials*, Vol. 14, No. 1, pp.014205, 2013.
- [7] M. A. A. Bash, A. M. Mustfa, A. M. Resan, F. F. Sayyid, "Microstructure and microhardness of laser cladding Ni based on cold rolled steel," *The Iraqi Journal for Mechanical and Materials Eng.*, Vol. 18, No. 2, pp. 201-213, 2018.

- [8] P. Chiu, J. Lin, "The Temperature Effects on the Microstructure and Profile in Laser Cladding," World Academy of Science, Eng. and Technology International Journal of Industrial and Manufacturing Eng. , Vol. 11, No. 10, pp. 1684-1688, 2017.
- [9] S. Tuncay, M. Izciler, "Laser cladding of hot work tool steel (H13) with TiC nanoparticles," Turkish Journal of Eng. (TUJE), Vol. 3, No. 1, pp. 25-31, 2019.
- [10] A. A. Moosa, M. J. Kadhim, A. Subhi, "Dilution effect during Laser Cladding of Inconel 617 with Ni-Al Powders," Modern Applied Science, Vol. 5, No.1, pp.50, 2011.
- [11] D. M. Goodarzi, J. Pekkarinen, A. Salminen, "Analysis of laser cladding process parameter influence on the clad bead geometry," Welding in the World, Vol. 61, No. 5, pp. 883-891, 2017.
- [12] M. J. kadhim, "Laser cladding of ceramics and sealing of plasma sprayed zirconia based thermal barrier coatings," PhD thesis, Dept. of Materials, Univ. of Imperial Collage, London, 1990.
- [13] Y. Huang, "Characterization of dilution action in laser-induction hybrid cladding," Optics & Laser Technology, Vol. 43, No. 5, pp. 965-973, 2011.
- [14] I. Manna, J. D. Majumdar, B. R. Chandra, S. Nayak, "Laser surface cladding of Fe-B-C, Fe-B-Si and Fe-BC-Si-Al-C on plain carbon steel," Surface and Coatings Technology, Vol. 201, No. 1-2, pp. 434-440, 2006.
- [15] A. J. Pinkerton, L. Li, "Modelling the geometry of a moving laser melt pool and deposition track via energy and mass balances," Journal of Physics D: Applied Physics, Vol. 37, No. 14, pp. 1885, 2004.